Journal of Multidisciplinary Engineering Science and Technology (JMEST)
ISSN: 2458-9403
Vol. 9 Issue 5, May - 2022

Exalted Thermoelectric Performances of Hematite (α-Fe_2O_3) Doped with Zn

Md. Ataur Rahman
Pundra University of Science & Technology
Bogura, Bangladesh
ataur4901@gmail.com

Abu Bakar Md. Ismail
University of Rajshahi
Rajshahi, Bangladesh
ismail@ru.ac.bd

***Abstract*— For renewable energy solution, in recent time, the thermoelectric technology has attracted much attention. In this research, the thermoelectric properties of Zn doped α-Fe_2O_3 (Zn:*α*-Fe_2O_3) was investigated. Fe_2O_3 is naturally n-type material. For making p-type Fe_2O_3, Zn doped Fe_2O_3 was developed. Zn doped Fe_2O_3 was successfully prepared via chemical synthesis. Due to the unique material properties and remarkable performance in electronic, photonics and optics, Zn was used. The band gap of α-Fe_2O_3 is quite low of for an oxide semiconductor (2.2 eV). The dimensionless figure of merit, *ZT*, of the 2 wt.% Zn doped α-Fe_2O_3 shows the higher value at 1150K. The conduction type was confirmed by Hall Effect measurement. In the temperature range of 300K to 1150K, the electrical conductivity and the Seebeck coefficient were measured by four-probe method. Under vacuum, in the same temperature range, the thermal conductivity was measured. The crystal structure was also studied by X-Ray Diffraction (XRD, Cu-Kα radiation) and Scanning Electron Microscopy (SEM). In this work, the produced p-type hematite exhibited excellent thermoelectric performance. Furthermore, the results figured that the thermoelectric properties of hematite had a remarkable effect on the thermoelectric technology as a renewable energy solution.**

Keywords— Hematite, Seebeck Coefficient, Electrical Conductivity, Thermal Conductivity, Figure of Merit

I. Introduction

In recent time, thermoelectric technology has made significant scientific progress and its potential to reduce the environmental impact of electrical power generation. Thermoelectric technology has attracted much attention as a renewable energy solution. In this technology heat is directly converted into electricity owing to temperature differences, and can act as power generators [1, 2]. The main focus of this research will be investigated thermoelectric properties by using Fe_2O_3 material. This material is used because of its low cost, abundance and do not require preparation to extremes of purity. Bi_2Te_3, PbTe and SiGe are currently popular as thermoelectric materials, however, these materials suffer drawbacks in that they are manufactured from expensive and toxic raw materials [3]. It is therefore important to develop alternative thermoelectric materials that are inexpensive and environmentally friendly. Iron oxides are such type of material which are earth abundant and environmentally friendly.

The performance of thermoelectric materials is evaluated by using the expression [4, 5],

$$ZT = \frac{S^2\sigma}{\kappa}T$$

Where, ZT is the figure of merit, S is the Seebeck coefficient, σ is the electrical conductivity, κ is the thermal conductivity and T is the absolute temperature.

Improving thermoelectric materials, significant progress has been made in recent years [6–18], however, in large-scale renewable energy conversion, the application of thermoelectrics has not been demonstrated [19]. The conventional sagacity is that thermoelectrics are most suitable for waste heat recovery and for large-scale applications that materials with significantly higher ZT are needed [1, 5, 20]. For converting heat energy into electricity, it will show that thermoelectrics are an attractive alternative.

The intention of this paper is to give a detailed studies of the electrical conductivity, thermal conductivity and the Seebeck coefficient. X-Ray Diffraction and Scanning Electron Microscopy (SEM) are also studied.

II. Experimental Details

Chemical synthesis process was used for preparation of Zn doped α-Fe_2O_3. For making p-type α-Fe_2O_3, Zn^{2+} dopant from Zinc acetate salt [$Zn(O_2CCH_3)_2$] was used.

The preparation of required samples is shown in Table 1, where the values of x are 0, 0.1, 0.5, 0.8, 1, 1.5 and 2. Then the solution was mixed and stirred at 35 minutes.

Table 1: Sample preparation

$FeCl_2$	Ethanol	(100-x) wt.% Fe_2O_3	x wt.% Zn (here x=2)
1.242 gm	10 ml	0.72 gm	0.048 gm

After that the resulting Zn doped Fe_2O_3 solution was prepared. For making Zn doped α-Fe_2O_3, the resulting solution was then sintered at 1073K for 4 hours. Then the powder form was produced. This powder was then pressed at 235 MPa, sintered at 1213 K, and finally annealed at 1043 K to give doped samples of α-Fe_2O_3. The conduction type was confirmed by Hall Effect measurement. From the result of Hall Effect measurement, Zn doped α-Fe_2O_3 was found to be p-type.

The electrical conductivity and the Seebeck coefficient were measured by four-probe method. Under vacuum, the thermal conductivity was measured. Microstructure analysis was performed by X-Ray Diffraction (XRD) with Cu-Kα (λ = 1.7902 Å) radiation in the 2θ range of 10-80º and Scanning Electron Microscopy (SEM).

III. Experimental Result and Discussion

A. X-Ray Diffraction (XRD) and Scanning Electron Microscopy (SEM)

The XRD patterns of Zn doped α-Fe_2O_3 with different doping concentrations are shown in Fig. 1.

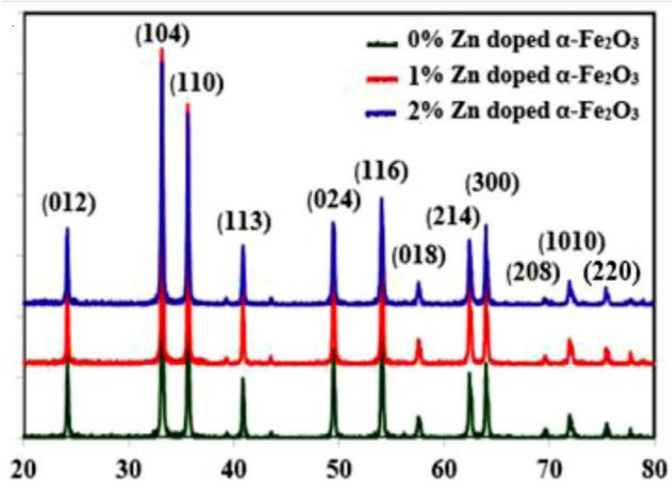

Fig. 1: XRD patterns of Zn doped α-Fe_2O_3 with different doping concentrations.

It is observed that all sharp peaks present with different crystal orientations are the planes of α-Fe_2O_3 [21, 22] which clearly show the polycrystalline nature. The regarded peaks can be indexed in agreement with the expected rhombohedral structure of α-Fe_2O_3 (space group: R-3c, ICDD card no. 33–0664) [23].

The SEM images of the sample are shown in Fig. 2 and used to study the morphology of the particles. The surface morphology of 2 wt.% Zn doped α-Fe_2O_3 indicate that it has slightly higher particle size than the others Zn doped α-Fe_2O_3 samples. From figure, it is seen that the presence of particles is more compact and has dense structure and the crystal quality is improved by increasing the Zn concentrations.

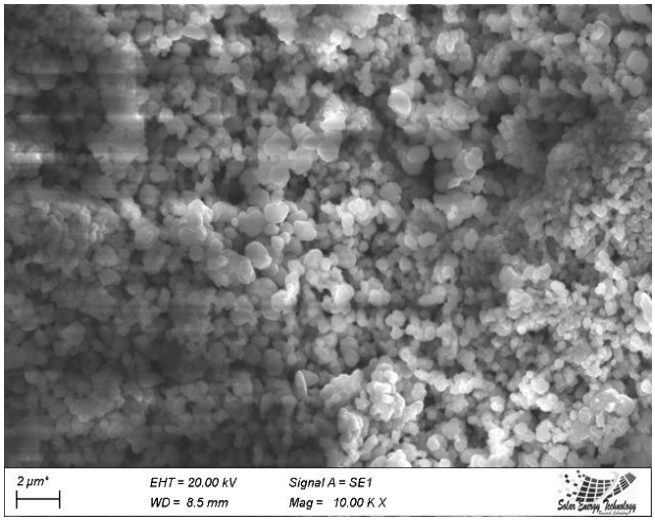

(a)

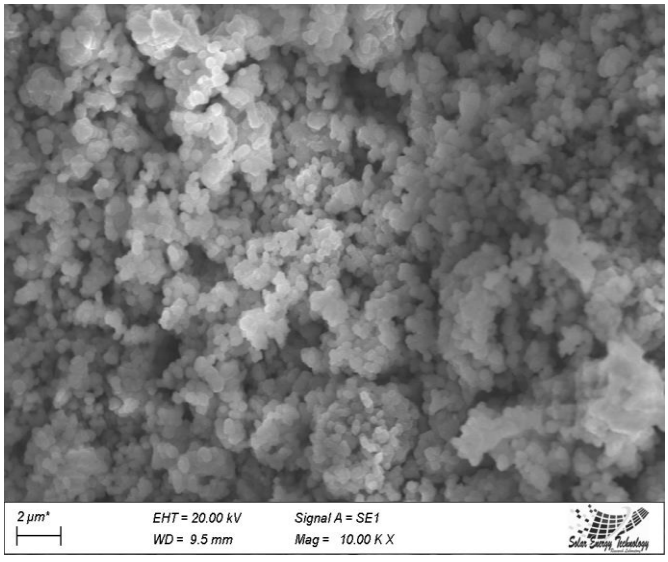

(b)

Fig. 2: SEM image of (a) 1 wt.% Zn doped α-Fe_2O_3 and (b) 2 wt.% Zn doped α-Fe_2O_3.

The presence of more Zn and interstitials/vacancies made the particle size of 2 wt.% Zn doped α-Fe_2O_3 sample higher than the samples 0%, 0.1%, 0.5%, 0.8%, 1% and 1.5% wt.% Zn doped α-Fe_2O_3. It is observed that, the samples have tightly packed grains with increased the Zn concentrations. This result indicates that Zn-doping has an influence on the surface morphology of the samples.

B. Seebeck coefficient and electrical conductivity

Fig. 3 shows the temperature dependences of the Seebeck coefficient for the samples of Zn doped α-Fe_2O_3 containing x wt.% of Zn. It is observed from the figure that, the Seebeck coefficient increased with increasing the values of x=1, 1.5 and 2 wt.% of Zn doped α-Fe_2O_3. On the other hand, the Seebeck coefficient, of the other values of x, exhibit intricate behaviors. From the figure it is seen that absolute values of the Seebeck coefficient increased with increasing the temperature.

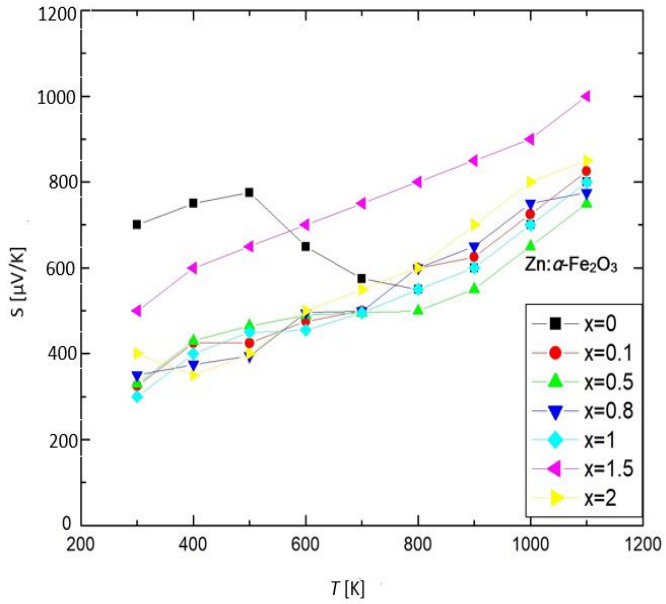

Fig. 3: The temperature dependences of the Seebeck coefficient for samples of Zn doped α-Fe_2O_3 containing x wt.% of Zn.

The temperature-dependent electrical conductivity of Zn doped α-Fe_2O_3 with different doping concentrations samples is shown in Fig. 4. From the figure, it is observed that, the addition of the Zn helped to increase the electrical conductivity. The cause of this increase in electrical conductivity i.e. the reduction in resistivity is believed to be the local deformation of the crystal caused by polarization of lattice, as a result of this lattice-induced polarization, electrons mobility is increased in the defects in the Zn doped-material.

Another effect of adding Zn is a slight tendency for the electrical conductivity to increase with increasing temperature. From the above discussion, we conclude that an increase in the absolute Seebeck coefficient and an increase in electrical conductivity i.e. a decrease in electrical resistivity with increasing temperature are auspicious for thermoelectric materials.

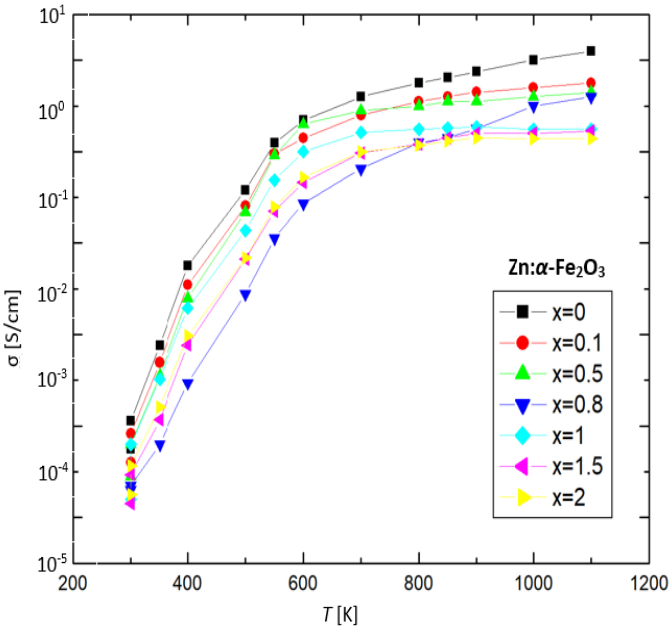

Fig. 4: The temperature dependences of the electrical conductivity for samples of Zn doped α-Fe_2O_3 containing x wt.% of Zn.

C. Thermal Conductivity

The temperature-dependent changes in thermal conductivity of Zn doped α-Fe_2O_3 with different doping concentrations samples is shown in Fig. 5. Thermal conductivity is also an important property of a thermoelectric material. The value of the thermal conductivity, κ, can be calculated from the following equation, which is based on the Wiedemann–Franz law [3, 24]:

$$L = \frac{\kappa_e}{\sigma T} = \frac{\pi^2}{3}\left(\frac{K_B}{e}\right)^2 = 2.44 \times 10^{-8}\, W\Omega K^{-2} \quad (1)$$

where, L is the Lorentz number, σ is the electrical conductivity, κ_e is the thermal conductivity due to electrons, K_B is the Boltzmann constant, and e is the charge on the electron.

The eq. (1) describes the thermal conductivity. The measured thermal conductivity is the sum of two parts κ_e and κ_{ph}, where κ_{ph} is the thermal conductivity due to lattice vibrations (i.e., phonons).

Due to the decrease in the phonon mean free path length, the temperature-dependent decrease occurred in the thermal conductivity. With increasing temperature, the phonon mean free path length linearly decreases.

Experimental results show that the contribution of thermal conductivity in the sample of 2 wt.% Zn doped α-Fe_2O_3 is relating to the electrical conductivity and Seebeck coefficient. So, the ratio of κ_{ph}/κ_e for 2 wt.% Zn doped α-Fe_2O_3 is lower than is the case for other samples leading to increases of the Seebeck coefficient and the electrical conductivity. From the above discussion, we concluded that the samples of Zn doped α-Fe_2O_3 containing different doping concentrations show the lower thermal conductivity which is better in thermoelectric performances of hematite.

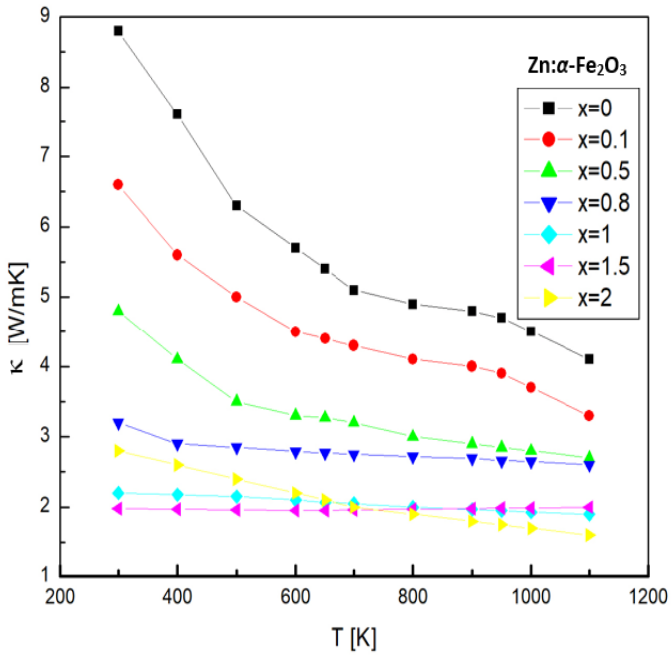

Fig. 5: The temperature dependences of the thermal conductivity for samples of Zn doped α-Fe_2O_3 containing x wt.% of Zn.

D. Figure of Merit

The thermoelectric performance is generally evaluated by means of the following equation [4, 5, 25, 26]:

$$ZT = \frac{S^2\sigma}{\kappa}T \qquad (2)$$

where, ZT is the dimensionless figure of merit, S is the Seebeck coefficient, σ is the electrical conductivity, κ is the thermal conductivity and T is the absolute temperature.

To evaluate the dimensionless figure of merit by the eq. (2), the value of ZT is can also be used as a measure of the performance of a thermoelectric material at the optimum temperature where the material shows its best performance. The thermoelectric properties of materials can be controlled by altering three properties simultaneously [27].

It is quite impossible to express the Seebeck coefficient in terms of a simple factor because, in addition to the energy gap, the interaction of electrons with phonons (polarons) may also play a role in thermoelectric power [3].

Due to temperature-dependent variations, the dimensionless figure of merit, *ZT*, of the Zn doped α-Fe_2O_3 is not very high as shown in Fig. 6. It is observed that the measured *ZT* values for the 2 wt.% Zn doped α-Fe_2O_3 is relatively higher than the other samples.

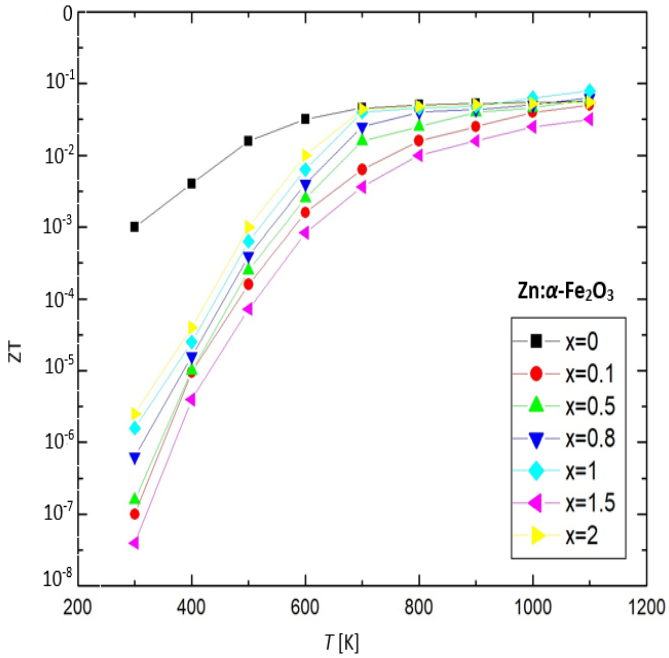

Fig. 6: The dimensionless figure of merit for samples of Zn doped α-Fe_2O_3 containing x wt.% of Zn.

IV. CONCLUSION

In summary, the temperature-dependent changes in the p-type iron oxide semiconductors, Zn doped α-Fe_2O_3 containing different doping concentrations are studied. The existence of planes of *α*-Fe_2O_3 and polycrystalline nature are confirmed by XRD study. From SEM study, it is observed that, with increased of the Zn concentrations, the samples have tightly packed grains.

The result of SEM study indicates that the surface morphology of the samples is influenced by Zn-doping. The temperature dependences of the Seebeck coefficient for the samples of Zn doped α-Fe_2O_3 containing 1, 1.5 and 2 wt.% of Zn exhibits excellent output. The temperature dependences of the electrical conductivity comprise the result which is showed that with increasing temperature, the electrical conductivity is increased.

At temperatures that are below 700K, The temperature-dependent changes in thermal conductivity of Zn doped α-Fe_2O_3 with different doping concentrations showed a dramatic decrease in the thermal conductivity.

The impurity scattering effect causes a significant decrease in the thermal conductivity. The dimensionless figure of merit, ZT, is relatively high for the 2 wt.% Zn doped α-Fe_2O_3. The addition of Zn in α-Fe_2O_3 resulted the best thermoelectric performance.

REFERENCES

[1] L. E. Bell, Cooling, heating, generating power, and recovering waste heat with thermoelectric systems, Science 2008**,** 321**,** 1457–1461**.**

[2] H. Edwards, Q. Niu, A. de Lozanne**,** Thermoelectric Conversion, in Wiley Encyclopedia of Electrical and Electronics Engineering (Ed.: J. G. Webster), Wiley-VCH, Weinheim, 1999.

[3] S. Sugihara, K. Morikawa, Improved Thermoelectric Performances of Oxide-Containing $FeSi_2$, Materials Transactions, 2011, 52, 1526-1530.

[4] H. J. Goldsmid, Thermoelectric Refrigeration, Plenum, 1964.

[5] D. M. Rowe, Thermoelectrics Handbook Nano to Macro, CRC Taylor & Francis, 2006.

[6] R. Venkatasubramanian, E. Siivola, T. Colpitts & B. O'Quinn, Thin-film thermoelectric devices with high room-temperature figures of merit. Nature 2001, 413, 597–602.

[7] T. C. Harman, P. J. Taylor, M. P. Walsh & B. E. LaForge, Quantum dot superlattice thermoelectric materials and devices. Science 2002, 297, 2229–2232.

[8] K. F. Hsu *et al*. Cubic AgPb*m*SbTe2C*m*: Bulk thermoelectric materials with high figure of merit. Science 2004, 303, 818–821.

[9] M. S. Dresselhaus *et al*. New directions for low-dimensional thermoelectric materials. Adv. Mater. 2007, 19, 1043–1053.

[10] B. Poudel *et al*. High-thermoelectric performance of nanostructured bismuth antimony telluride bulk alloys. Science 2008, 320, 634–638.

[11] J. P. Heremans, *et al*. Enhancement of thermoelectric efficiency in PbTe by distortion of the electronic density of states. Science 2008, 321, 554–557.

[12] A. I. Boukai *et al*. Silicon nanowires as efficient thermoelectric materials. Nature 2008, 451, 168–171.

[13] A. I. Hochbaum *et al*. Enhanced thermoelectric performance of rough silicon nanowires. Nature 2008, 451, 163–167.

[14] G. J. Snyder & E. S. Toberer, Complex thermoelectric materials. Nature Mater. 2008, 7, 105–114.

[15] J. S. Rhyee *et al*. Peierls distortion as a route to high thermoelectric performance in In_4Se_3-delta crystals. Nature 2009, 459, 965–968.

[16] X. B. Zhao *et al*. Bismuth telluride nanotubes and the effects on the thermoelectric properties of nanotube-containing nanocomposites. Appl. Phys. Lett. 2005, 86, 062111.

[17] X. F. Tang, *et al*. Preparation and thermoelectric transport properties of high-performance p-type Bi_2Te_3 with layered nanostructure. Appl. Phys. Lett. 2007, 90, 012102.

[18] T. M. Tritt & M. A. Subramanian, Energy harvesting through thermoelectrics: Power generation and cooling. MRS Bull. 2006, 31, 188–194.

[19] C. B. Vining, An inconvenient truth about thermoelectrics. Nature Mater. 2009, 8, 83–85.

[20] J. H. Yang & F. R. Stabler, Automotive applications of thermoelectric materials. J. Electron. Mater. 2009, 38, 1245–1251.

[21] J. Hua, J. Gengsheng, Hydrothermal synthesis and characterization of. monodisperse *α*-Fe_2O_3 nanoparticles, Mater. Lett. 2009, 63, 2725–2727.

[22] T. Almeida, M. Fay, Y.Q. Zhu, P. D. Brown, Process map for the hydrothermal synthesis of *α*-Fe_2O_3 nanorods, J. Phys. Chem. C 2009, 113, 18689–18698.

[23] A. Lassoued, Synthesis and characterization of Zn-doped α-Fe_2O_3 nanoparticles with enhanced photocatalytic activities, Journal of Molecular Structure 2021, 1239, 130489.

[24] A. Yadav *et al,* An analytic study of the Wiedemann–Franz law and the thermoelectric figure of merit, J. Phys. Commun. 2019, 3, 105001.

[25] G. Mahan, B. Sales and J. Sharp, Thermoelectric Materials: New Approaches to an Old Problem, Phys. Today 1997, 50, 42-47.

[26] H. J. Goldsmid & D.M. Rowe, CRC Handbook of Thermoelectrics, CRC Press, 1995.

[27] S. Sugihara, K. Nishiyama, Y. Igarashi and K. Morikawa, Chapter 18-Functions of Metal Oxide for Thermoelectric Materials and Electronic Structures, Adv. Quantum Chem. 2008, 54, 227-243.